

Heralded quantum repeater based on the scattering of photons off single emitters in weak-coupling regime

Guo-Zhu Song, Mei Zhang, Qing Ai, Guo-Jian Yang, and Fu-Guo Deng*

*Department of Physics, Applied Optics Beijing Area Major Laboratory,
Beijing Normal University, Beijing 100875, China*

(Dated: November 21, 2018)

We propose a heralded quantum repeater based on the scattering of photons off single emitters in one-dimensional waveguides. We show the details by implementing nonlocal entanglement generation, entanglement swapping, and entanglement purification modules with atoms in waveguides, and discuss the feasibility of the repeater with currently achievable technology. The scheme features a filtering mechanism that the faulty events can be discarded by detecting the polarization of the photons. That is, our protocols either succeed with 100% fidelity or fail in a heralded way, which is advantageous for implementing realistic long-distance quantum communication. Moreover, additional atomic qubits are not required, but only a single-photon medium. Our scheme is scalable and attractive since it can be realized in solid-state quantum systems. With the great progress on controlling atom-waveguide systems, this repeater may be very useful in quantum information processing in the future.

PACS numbers: 03.67.Pp, 03.67.Bg, 03.67.Hk, 42.50.Pq

I. INTRODUCTION

An important task of quantum communication is to transmit information between distant parties securely, such as quantum key distribution [1–3], quantum secret sharing [4–6], and quantum secure direct communication [7–9]. The creation of long-distance entanglement plays an important role in quantum communication. In order to exchange private information and avoid an exponential decay of photons over long distance, the scheme for quantum repeater was proposed by Briegel *et al.* [10] in 1998. Its main idea is to generate the entangled pairs in small segments first, avoiding the exponential decay of photons with the transmission distance, and then use entanglement swapping [11] and entanglement purification [12, 13] to create a long-distance entangled quantum channel.

There are some interesting proposals for implementing a quantum repeater, by utilizing different physical systems. For example, in 2001, Duan *et al.* [14] suggested an original proposal to set up a quantum repeater with atomic ensembles, called it the Duan-Lukin-Cirac-Zoller (DLCZ) protocol. It exploits atomic ensembles as quantum memories, and Raman transitions in atomic ensembles are used to produce the nonclassical correlation between atomic excitations and emitted photons. In 2006, Klein *et al.* [15] put forward a robust scheme for quantum repeaters with decoherence-free subspaces. In 2007, using the two-photon Hong-Ou-Mandel interferometer, Zhao *et al.* [16] proposed a robust quantum repeater protocol. In 2012, Wang, Song, and Long [17] presented an efficient scheme for robust quantum repeaters based on spatial entanglement of photons and quantum-dot spins in optical microcavities. In 2015, Li and Deng [18] pre-

sented a heralded high-efficiency quantum repeater with atomic ensembles assisted by faithful single-photon transmission. Later, Li, Yang, and Deng introduced another heralded quantum repeater for quantum communication network based on quantum dots embedded in optical microcavities, resorting to effective time-bin encoding [19]. The building blocks of quantum repeaters are experimentally realized by some research groups, and remarkable progress has been reported [20–24].

In the past decade, the interaction between photons and atoms in high-quality optical microcavities has become one of the most important methods for implementing quantum computation and quantum information processing. Some significant achievements [25–29] have been made in photon-atom systems in both theory and experiment. With strong coupling and high-quality cavities, they can obtain a high-fidelity quantum computation. In 2005, an interesting proposal [30] was proposed to realize the coupling between a single quantum emitter and a photon in one-dimensional (1D) waveguides, which can be considered as a bad cavity. In their scheme, the coupling between the emitter and the cavity is stronger than the atomic decay rate, but weaker than the cavity-loss rate, and the atomic spontaneous emission into the waveguide becomes the main effect, called the Purcell effect. In 2007, a similar proposal was presented to realize this coupling using nanoscale surface plasmons [31]. It is worth noting that the significant nonlinear optical property can still be obtained in the weak-coupling regime (low- Q regime).

In contrast to strong-coupling regime, the weak-coupling regime is less technically demanding and still allows for interesting quantum state manipulation and quantum information processing, such as entanglement generation [32–34], efficient optical switch [35], quantum logic gates [36], and quantum state transfer [37–39]. However, with emitter decay and finite coupling strength,

*Corresponding author: fgdeng@bnu.edu.cn

the physical device is restricted to finite P (Purcell factor), so that the scattering of photons off single emitters may not happen at all. To solve this problem, in 2012, Li *et al.* [39] proposed a simple scattering setup to realize a high-fidelity Z gate on an atom assisted by a single-photon medium, in which the faulty events can be heralded by detecting the polarization of the photon pulse.

In this paper, we present a heralded quantum repeater that allows the creation of the entangled state over an arbitrary large distance with a tolerability of errors. In our scheme, since atoms can provide long coherence time, we choose a four-level atom as the emitter. With the scattering of photons off single emitters in 1D waveguides, the parties in quantum communication can realize nonlocal entanglement creation against collective noise, entanglement swapping, and entanglement purification. Moreover, our protocols can turn errors into the detection of photon polarization, which can be discarded. The prediction of faulty events ensures that our repeater either succeeds with perfect fidelity or fails in a heralded way, which is advantageous for quantum information processing.

The paper is organized as follows: In Sec. II, we introduce the transport property of a photon scattering with a two-level atom coupled to a 1D waveguide, and then show the protocols for implementing nonlocal entanglement creation, entanglement swapping, and entanglement purification. In Sec. III, we discuss a few relevant issues related to the implementation of our repeater in a realistic system, and end up with a summary.

II. QUANTUM REPEATER BASED ON THE SCATTERING CONFIGURATION

A. The scattering of photons off single emitters in a 1D waveguide

Let us consider a quantum system composed of a single emitter coupled to electromagnetic modes in a 1D waveguide, as shown in Fig. 1(a). We first choose a simple two-level atom as the emitter, consisting of the ground state $|g\rangle$ and the excited state $|e\rangle$ with the frequency difference ω_a . Under the Jaynes-Cummings model, the Hamiltonian for the interactions between a set of waveguide modes and a two-level atom reads:

$$H = \sum_k \hbar \omega_k a_k^\dagger a_k + \frac{1}{2} \hbar \omega_a \sigma_z + \sum_k \hbar g (a_k^\dagger \sigma_- + a_k \sigma_+), \quad (1)$$

where a_k and a_k^\dagger are the annihilation and creation operators of the waveguide mode with frequency ω_k , respectively. σ_z , σ_+ , and σ_- are the inversion, raising, and lowering operators of the two-level atom, respectively. g is the coupling strength between the atom and the electromagnetic modes of the 1D waveguide, assumed to be same for all modes. One can rewrite the Hamiltonian of

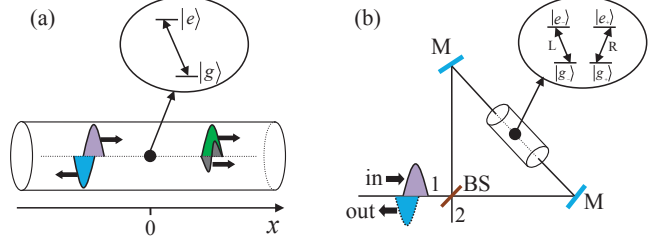


FIG. 1: (a) The basic structure for a photon mirror in which a two-level atom (an emitter marked by the black dot) is coupled to a 1D waveguide (marked by the cylinder). Here the atom has a ground state $|g\rangle$ and an excited state $|e\rangle$, and its position is $x = 0$. In an ideal situation, an incident photon (purple, the upper left wave packet) is fully reflected (blue, the lower left wave packet) when it resonates with the atom, but there is a transmitted component (black, the right wave packet) in a practical scattering. Note that, having no connection with the emitter, the incident photon goes through the atom with no effect (green, the upper right wave packet). (b) A heralded setup to realize a high-fidelity Z gate on an atom in the 1D waveguide. Different from the emitter in Fig. 1(a), the atom has two degenerate ground states $|g_{\pm}\rangle$ and two degenerate excited states $|e_{\pm}\rangle$ coupled to the waveguide (marked by the cylinder). BS is a 50 : 50 beam splitter, M is a fully reflected mirror, and the black lines represent the paths of the traveling photon.

the system in real space as

$$H' = \hbar \int dk \omega_k a_k^\dagger a_k + \hbar g \int dk (a_k \sigma_+ e^{ikx_a} + h.c.) + \hbar (\omega_a - \frac{i\gamma'}{2}) \sigma_{ee}, \quad (2)$$

where x_a is the position of the atom, $\sigma_{ee} = |e\rangle\langle e|$, and $\omega_k = c|k|$ (c is the group velocity of the propagating electromagnetic modes and k is its wave vector). γ' is the decay rate of the atom out of the waveguide (e.g., the emission into the free space). Because we only care the interactions of the near-resonant photons with the atom, we could make the approximation that left- and right-propagating photons form completely separate quantum fields [30]. Under this approximation, the operator a_k in Eq. (2) can be replaced by $(a_{k,R} + a_{k,L})$.

To get the reflection and transmission coefficients of single-photon scattering, we assume that a photon with the energy E_k is propagating from the left. The state of the system is described by

$$|E_k\rangle = c_e |e, vac\rangle + \int dx [\phi_L(x) c_L^\dagger(x) + \phi_R(x) c_R^\dagger(x)] |g, vac\rangle, \quad (3)$$

where $|vac\rangle$ represents the vacuum state of photons, c_e is the probability amplitude of the atom in the excited state, and $c_L^\dagger(x)$ ($c_R^\dagger(x)$) is a bosonic operator creating a left-going (right-going) photon at position x . $\phi_R(x)$ and $\phi_L(x)$ are the probability amplitudes of right- and

left-traveling photon, respectively. Note that the photon propagates from the left, $\phi_R(x)$ and $\phi_L(x)$ could take the forms

$$\begin{aligned}\phi_R(x) &= e^{ikx}\theta(-x) + te^{ikx}\theta(x), \\ \phi_L(x) &= re^{-ikx}\theta(-x).\end{aligned}\quad (4)$$

Here t and r are the transmission and reflection coefficients, respectively. The Heaviside step function $\theta(x)$ equals 1 when x is larger than zero and 0 when x is smaller than zero. By solving the time-independent Schrödinger equation $H|E_k\rangle = E_k|E_k\rangle$, one can obtain

$$\begin{aligned}r &= -\frac{1}{1 + \gamma'/\gamma_{1D} - 2i\Delta/\gamma_{1D}}, \\ t &= 1 + r,\end{aligned}\quad (5)$$

where $\Delta = \omega_k - \omega_a$ is the photon detuning with the two-level atom, and $\gamma_{1D} = 4\pi g^2/c$ is the decay rate of the atom into the waveguide.

Provided that the incident photon resonates with the emitter (i.e., $\Delta = 0$), one can easily obtain the reflection coefficient $r = -1/(1 + 1/P)$, where $P = \gamma_{1D}/\gamma'$ is the Purcell factor. As we know, in the atom-waveguide system, the spontaneous emission rate γ_{1D} into the 1D waveguide can be much larger than the emission rate γ' into all other possible channels [30, 31]. Considering that the Purcell factor P can exceed 10^3 in realistic systems [31], one can get the reflection coefficient $r = -1$ for this system. That is, when the photon is coupled to the emitter, the atom acts as a photon mirror [30], which puts a π -phase shift on reflection. However, when the photon is decoupled from the emitter, it transmits through the atom with no effect.

Let us consider a four-level atom with the degenerate ground states $|g_{\pm}\rangle$ and excited states $|e_{\pm}\rangle$ as the emitter in a 1D waveguide, as shown in Fig. 1(b). For the emitter, the transitions of $|g_+\rangle \leftrightarrow |e_+\rangle$ and $|g_-\rangle \leftrightarrow |e_-\rangle$ are coupled to the two electromagnetic modes $a_{k,R}$ and $a_{k,L}$, with the absorption (or emission) of right (R) and left (L) circular polarization photons, respectively. Assuming that the spatial wave function of the incident photon is $|\psi\rangle$, with the scattering properties in the practical situation discussed above, one can get

$$\begin{aligned}|g_+\rangle|\psi\rangle|R\rangle &\rightarrow |g_+\rangle|\phi\rangle|R\rangle, \\ |g_-\rangle|\psi\rangle|L\rangle &\rightarrow |g_-\rangle|\phi\rangle|L\rangle, \\ |g_-\rangle|\psi\rangle|R\rangle &\rightarrow |g_-\rangle|\psi\rangle|R\rangle, \\ |g_+\rangle|\psi\rangle|L\rangle &\rightarrow |g_+\rangle|\psi\rangle|L\rangle.\end{aligned}\quad (6)$$

Here $|\phi\rangle$ is the spatial state of the photon component left in the waveguide after the scattering process. In practice, there is always a transmitted part [31], thus $|\phi\rangle = |\phi_t\rangle + |\phi_r\rangle$, where $|\phi_t\rangle$ and $|\phi_r\rangle$ refer to the transmitted and reflected parts of the photon, respectively. When the Purcell factor P is infinite, $|\phi\rangle$ is normalized. Whereas, if the input photon is in the horizontal linear-polarization state $|H\rangle = (|R\rangle + |L\rangle)/\sqrt{2}$, the transformations turn

into

$$\begin{aligned}|g_+\rangle|\psi\rangle|H\rangle &\rightarrow |g_+\rangle|\phi_t\rangle|H\rangle + |g_+\rangle|\phi_r\rangle|V\rangle, \\ |g_-\rangle|\psi\rangle|H\rangle &\rightarrow |g_-\rangle|\phi_t\rangle|H\rangle - |g_-\rangle|\phi_r\rangle|V\rangle,\end{aligned}\quad (7)$$

where $|V\rangle = (|R\rangle - |L\rangle)/\sqrt{2}$ is the vertical linear-polarization state of photons. It is interesting that the scattering process generates a vertical-polarized component, with which a heralded setup can be constructed to realize a high-fidelity Z gate on an atom, as shown in Fig. 1(b), similar to that in Ref. [39].

The input photon in spatial state $|\psi\rangle$ with $|H\rangle$ or $|V\rangle$ (from port 1) is split by a 50 : 50 beam splitter (BS) into two halves that scatter with the atom simultaneously. Then, the transmitted and reflected components travel back and exit the beam splitter from port 1. Note that, due to quantum destructive interference, there is no photon component coming out from port 2. Finally, discarding the output with unchanged photon polarization (i.e., the faulty events), one can get the high-fidelity Z_a gate as follows:

$$\begin{aligned}|\mu\rangle_a|\psi\rangle|H\rangle &\rightarrow -Z_a|\mu\rangle_a|\phi_r\rangle|V\rangle, \\ |\mu\rangle_a|\psi\rangle|V\rangle &\rightarrow -Z_a|\mu\rangle_a|\phi_r\rangle|H\rangle,\end{aligned}\quad (8)$$

where $|\mu\rangle_a$ is an arbitrary superposition state of the atom in the basis $\{|0\rangle_a \equiv |g_-\rangle, |1\rangle_a \equiv |g_+\rangle\}$. As mentioned above, $|\phi_r\rangle$ is the spatial wave function of the reflected photon component after the scattering process, as shown in Fig. 1(a). When $P \rightarrow \infty$, the perfect scattering process leads to $|\phi_r\rangle = -|\psi\rangle$. In the imperfect situation with a finite P , we get $|\phi_r\rangle \neq -|\psi\rangle$, the output photon with unchanged polarization is detected and the corresponding gate fails, which can be discarded. That is, the setup works for the Z gate on an atom in a heralded way.

B. Robust entanglement creation against collective noise

With the scattering property of a photon scattering with a four-level atom coupled to a 1D waveguide, we can design a robust scheme for the entanglement creation on two nonlocal stationary atoms a and b , as shown in Fig. 2. Suppose that the single photon medium and the two stationary atoms in 1D waveguides are initially prepared in the superposition states $|\psi_0\rangle^{ph} = \frac{1}{\sqrt{2}}(|H\rangle + |V\rangle)$ and $|\varphi_i\rangle = \frac{1}{\sqrt{2}}(|0\rangle + |1\rangle)_i$ (here $i = a, b$), respectively, and the state of the system composed of the photon and the two atoms is

$$|\Omega_0\rangle = \frac{1}{2\sqrt{2}}(|H\rangle + |V\rangle) \otimes (|0\rangle + |1\rangle)_a \otimes (|0\rangle + |1\rangle)_b. \quad (9)$$

Our scheme works with the following steps.

First, the $|H\rangle$ and $|V\rangle$ components of the input photon are spatially split by a polarizing beam splitter (PBS). In detail, the photon in state $|H\rangle$ passes through both PBS_1 and PBS_2 towards the setup to scatter with atom

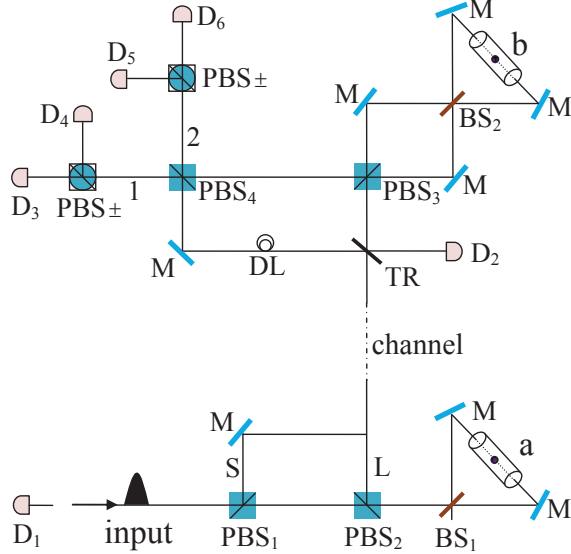


FIG. 2: Schematic setup for the creation of maximally entangled states on two nonlocal atoms a and b in 1D waveguides. PBS_i ($i = 1, 2, 3, 4$) represents a polarizing beam splitter which transmits the horizontal polarized photon $|H\rangle$ and reflects the vertical polarized photon $|V\rangle$. $PBS\pm$ transmits photons with polarization $|+\rangle$ and reflects photons with polarization $|-\rangle$, where $|\pm\rangle = (|H\rangle \pm |V\rangle)/\sqrt{2}$. D_i ($i = 1, 2, \dots, 6$) is a single-photon detector and DL is a time-delay device. TR is an optical device which can be controlled exactly as needed to transmit or reflect a photon.

a , while the component in state $|V\rangle$ is reflected and goes directly to the channel, having no interaction with atom a . After the scattering process, the part interacting with atom a enters into the channel, but a little later than the other part. The state of the whole system at the entrance of the channel becomes $|\Omega_1\rangle$. Here

$$\begin{aligned} |\Omega_1\rangle &= |\Omega_{1S}\rangle + |\Omega_{1L}\rangle, \\ |\Omega_{1S}\rangle &= \frac{1}{2\sqrt{2}}|V\rangle \otimes (|0\rangle + |1\rangle)_a \otimes (|0\rangle + |1\rangle)_b, \\ |\Omega_{1L}\rangle &= \frac{1}{2\sqrt{2}}|V\rangle \otimes (|0\rangle - |1\rangle)_a \otimes (|0\rangle + |1\rangle)_b, \end{aligned} \quad (10)$$

where $|\Omega_{1S}\rangle$ and $|\Omega_{1L}\rangle$ represent the two parts of the photon going through the short path (S) and the long path (L) to the channel, respectively.

Second, as the two parts in the channel are near and their polarization states are both in $|V\rangle$, the influences of the collective noise in the quantum channel on these two parts are the same one [40–43], which can be described by

$$|V\rangle \rightarrow \gamma|V\rangle + \delta|H\rangle, \quad (11)$$

where $|\gamma|^2 + |\delta|^2 = 1$. After the photon travels in the long quantum channel, the state of the whole system at

the output port becomes

$$\begin{aligned} |\Omega_2\rangle &= |\Omega_{2S}\rangle + |\Omega_{2L}\rangle, \\ |\Omega_{2S}\rangle &= \frac{1}{2\sqrt{2}}(\gamma|V\rangle + \delta|H\rangle)(|0\rangle + |1\rangle)_a(|0\rangle + |1\rangle)_b, \\ |\Omega_{2L}\rangle &= \frac{1}{2\sqrt{2}}(\gamma|V\rangle + \delta|H\rangle)(|0\rangle - |1\rangle)_a(|0\rangle + |1\rangle)_b. \end{aligned} \quad (12)$$

Third, coming out from the noisy channel, the early part of the photon in state $|\Omega_{2S}\rangle$ is reflected by the optical device TR and goes through a time-delay device, while the late part in state $|\Omega_{2L}\rangle$ transmits through TR into PBS_3 . After that, the components in $|H\rangle$ and $|V\rangle$ of the late part are split into two halves that scatter with atom b and travel back to PBS_3 simultaneously. Subsequently, the early part and the late part are rejoined in PBS_4 , and they are separated into two paths 1 and 2. The state of the whole system evolves into

$$\begin{aligned} |\Omega_3\rangle &= \frac{1}{2\sqrt{2}}\gamma(|H\rangle + |V\rangle)_1(|0\rangle|0\rangle + |1\rangle|1\rangle)_{ab} \\ &\quad - \frac{1}{2\sqrt{2}}\gamma(|H\rangle - |V\rangle)_1(|0\rangle|1\rangle + |1\rangle|0\rangle)_{ab} \\ &\quad + \frac{1}{2\sqrt{2}}\delta(|H\rangle + |V\rangle)_2(|0\rangle|0\rangle + |1\rangle|1\rangle)_{ab} \\ &\quad + \frac{1}{2\sqrt{2}}\delta(|H\rangle - |V\rangle)_2(|0\rangle|1\rangle + |1\rangle|0\rangle)_{ab}. \end{aligned} \quad (13)$$

Finally, the two parts in paths 1 and 2 go through $PBS\pm$, and the photon is detected by one of the four single-photon detectors D_3 , D_4 , D_5 , and D_6 . If the detector D_4 or D_5 clicks, we should put a σ_x operation on atom b . If the detector D_3 or D_6 clicks, nothing needs to be done. Eventually, the state of the system composed of atoms a and b collapses to the maximally entangled state

$$|\phi^+\rangle_{ab} = \frac{1}{\sqrt{2}}(|0\rangle|0\rangle + |1\rangle|1\rangle)_{ab}. \quad (14)$$

Our setup for the robust entanglement creation on two nonlocal atoms has some interesting features. First, the early part and the late part of the photon in the channel are so near that they suffer from the same collective noise [3, 40–43], and an arbitrary qubit error caused by the long noisy channel can be perfectly settled. Second, the faulty interactions between the photon and two atoms can be heralded by the detectors D_1 and D_2 . In detail, if one of the two detectors clicks, the event of the entanglement creation fails, which can be discarded. Moreover, the photon loss in the long quantum channel can be heralded by the photon detectors D_3 , D_4 , D_5 , and D_6 . Third, the probability of the entanglement creation is independent of the noise parameters. These good features make our setup have good applications in quantum repeaters for long-distance quantum communication.

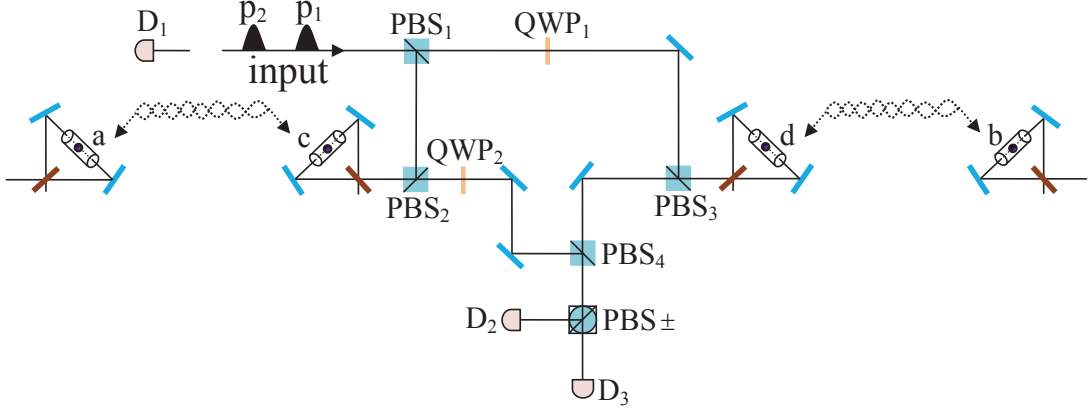


FIG. 3: Schematic diagram showing the principle of entanglement swapping. QWP_i ($i = 1, 2$) represents a quarter-wave plate, which is used to implement the conversion of the photon polarization.

C. Entanglement swapping

The atomic entangled state can be connected to longer communication distance via local entanglement swapping. As shown in Fig. 3, the two pairs of nonlocal atoms ac and bd are both initially prepared in the maximally entangled states $|\phi^+\rangle_{ac} = \frac{1}{\sqrt{2}}(|0\rangle|0\rangle + |1\rangle|1\rangle)_{ac}$ and $|\phi^+\rangle_{bd} = \frac{1}{\sqrt{2}}(|0\rangle|0\rangle + |1\rangle|1\rangle)_{bd}$, respectively. With the Bell-state measurement on local atoms cd and single-qubit operations, the two nonlocal atoms ab can collapse to the maximally entangled state $|\phi^+\rangle_{ab} = \frac{1}{\sqrt{2}}(|0\rangle|0\rangle + |1\rangle|1\rangle)_{ab}$, which indicates that the nonlocal entanglement for a longer communication is realized. The principle of quantum swapping is shown in Fig. 3, and the details are described as follows.

First, suppose that the input photon p_1 is prepared in the superposition state $|\psi\rangle^{p_1} = \frac{1}{\sqrt{2}}(|H\rangle + |V\rangle)_{p_1}$, and the initial state of the whole system composed of photon p_1 and the four atoms $acbd$ is $|\Psi_0\rangle$. Here

$$|\Psi_0\rangle = \frac{1}{2\sqrt{2}}(|H\rangle + |V\rangle)_{p_1} \otimes (|0\rangle|0\rangle + |1\rangle|1\rangle)_{ac} \otimes (|0\rangle|0\rangle + |1\rangle|1\rangle)_{bd}. \quad (15)$$

The injecting photon p_1 passes through PBS_1 , which transmits the photon in state $|H\rangle$ and reflects the photon in state $|V\rangle$. The photon in state $|V\rangle$ is reflected by PBS_1 and PBS_2 into the scattering setup composed of atom c , while the other part in state $|H\rangle$ goes through QWP_1 and is reflected by PBS_3 into the scattering setup to scatter with atom d . Then, the two parts of the photon p_1 are rejoined in PBS_4 and travel through $PBS\pm$. After that, the state of the whole system is changed from $|\Psi_0\rangle$ to

$|\Psi_1\rangle$. Here,

$$|\Psi_1\rangle = \frac{(|H\rangle + |V\rangle)_{p_1}}{4\sqrt{2}} [(|00\rangle - |11\rangle)_{cd} \otimes (|00\rangle + |11\rangle)_{ab} + (|00\rangle + |11\rangle)_{cd} \otimes (|00\rangle - |11\rangle)_{ab} - \frac{(|H\rangle - |V\rangle)_{p_1}}{4\sqrt{2}} [(|01\rangle - |10\rangle)_{cd} \otimes (|01\rangle + |10\rangle)_{ab} + (|01\rangle + |10\rangle)_{cd} \otimes (|01\rangle - |10\rangle)_{ab}]. \quad (16)$$

The first and the second parts of the photon in Eq. (16) are detected by the detectors D_3 and D_2 , respectively.

Second, after the measurement on photon p_1 , a Hadamard operation H_a (e.g., using a $\pi/2$ microwave pulse or optical pulse [44, 45]) is performed on the two local atoms c and d in the waveguides, respectively. Subsequently, we input another photon p_2 into the setup, which is initially prepared in the state $\frac{1}{\sqrt{2}}(|H\rangle + |V\rangle)_{p_2}$. Photon p_2 has the same process as photon p_1 , for simplicity, we omit the process of photon p_2 . When the two parts of photon p_2 arrive in PBS_4 simultaneously, the state of the whole system becomes

$$|\Psi_2\rangle = \frac{(|H\rangle + |V\rangle)_{p_2}}{4\sqrt{2}} [(|00\rangle - |11\rangle)_{cd} \otimes (|00\rangle - |11\rangle)_{ab} - (|00\rangle + |11\rangle)_{cd} \otimes (|01\rangle - |10\rangle)_{ab} - \frac{(|H\rangle - |V\rangle)_{p_2}}{4\sqrt{2}} [(|01\rangle - |10\rangle)_{cd} \otimes (|00\rangle + |11\rangle)_{ab} + (|01\rangle + |10\rangle)_{cd} \otimes (|01\rangle + |10\rangle)_{ab}]. \quad (17)$$

Then, photon p_2 travels through the $PBS\pm$ and is detected. If the photon detector D_3 clicks, it corresponds to the first part in Eq. (17). If D_2 clicks, it means the second part in Eq. (17) is probed.

Third, with the outcomes of the detectors for photons p_1 and p_2 , one can see that the four Bell states of the

atoms a and b are completely distinguished. Finally, the parties can perform corresponding operations (see Table I) on atom a to complete the quantum swapping. After that, the state of the two nonlocal atoms a and b in a longer distance collapses to the maximally entangled state $|\phi^+\rangle_{ab}$.

It is important to note that the wrong interactions between photon and atoms are heralded by the photon detectors for the quantum swapping in our scheme. In detail, if detector D_1 clicks, the interactions between photon and two atoms in 1D waveguides are faulty, which could be discarded. If detector D_2 or D_3 does not click, the photon loss occurs during the whole process. Therefore, with the prediction of the faulty events, the parties can obtain a high-fidelity nonlocal atomic entangled state in a longer distance.

TABLE I: The operations on atom a corresponding to the outcomes of the photon detectors D_2 and D_3 .

First click	Second click	Operations on atom a
D_3	D_2	I
D_3	D_3	σ_z
D_2	D_2	σ_x
D_2	D_3	$\sigma_z\sigma_x$

D. Entanglement purification

In Sec. II B and Sec. II C, we only talk about the influence of noise on flying photons in long quantum channel. In the practical situation, the errors also occur in stationary atoms embedded in 1D waveguides, which will decrease the entanglement of the nonlocal two-atom systems. Using entanglement purification, we can distill some high-fidelity maximally entangled states from a mixed entangled state ensemble.

Now, we start to explain the principle of our purification protocol for nonlocal atomic entangled states, assisted by the scattering of photons off single atoms in 1D waveguides, as shown in Fig. 4.

Suppose that the initial mixed state shared by two remote parties, say Alice and Bob, can be written as

$$\rho_{ab} = F|\phi^+\rangle_{ab}\langle\phi^+| + (1-F)|\psi^+\rangle_{ab}\langle\psi^+|, \quad (18)$$

where $|\psi^+\rangle_{ab} = \frac{1}{\sqrt{2}}(|0\rangle|1\rangle + |1\rangle|0\rangle)_{ab}$. The subscripts a and b represent the single atoms in 1D waveguides owned by the two parties Alice and Bob, respectively. F is the initial fidelity of the state $|\phi^+\rangle$. By selecting two pairs of nonlocal entangled two-atom systems, the four atoms are in the states $|\phi^+\rangle_{a_1b_1}|\phi^+\rangle_{a_2b_2}$ with the probability of F^2 , $|\phi^+\rangle_{a_1b_1}|\psi^+\rangle_{a_2b_2}$ and $|\psi^+\rangle_{a_1b_1}|\phi^+\rangle_{a_2b_2}$ with a probability of $F(1-F)$, and $|\psi^+\rangle_{a_1b_1}|\psi^+\rangle_{a_2b_2}$ with a probability of $(1-F)^2$, respectively. Our entanglement purification protocol for nonlocal entangled atom pairs works with the following steps.

First, both Alice and Bob prepare an optical pulse in the superposition state $\frac{1}{\sqrt{2}}(|H\rangle + |V\rangle)$ and let their pulses pass through the equipments shown in Fig. 4. To simplify the discussion, we just discuss the interactions in Alice, and Bob need complete the same process simultaneously. For Alice, the $|H\rangle$ and $|V\rangle$ components of the input photon 1 are spatially split by PBS_1 . In detail, the component in $|V\rangle$ is reflected by both PBS_1 and PBS_2 to the scattering setup composed of atom a_1 , whereas the component in $|H\rangle$ goes through QWP_2 and is reflected by PBS_3 to the scattering setup containing atom a_1 . Subsequently, the two parts of photon 1 are rejoined at PBS_4 and travel through $PBS\pm$. Meanwhile, another photon 2 has the same process as photon 1 simultaneously.

Second, after the above interactions, photon 1 and photon 2 are probed by single-photon detectors and there are two kinds of measurement results. In detail, if the two pairs of nonlocal two-atom systems are initially in the state $|\phi^+\rangle_{a_1b_1}|\phi^+\rangle_{a_2b_2}$, the evolution of the whole system is

$$\begin{aligned} & \frac{1}{4}(|H\rangle + |V\rangle)_1(|H\rangle + |V\rangle)_2(|00\rangle + |11\rangle)_{a_1b_1}(|00\rangle + |11\rangle)_{a_2b_2} \\ & \rightarrow \frac{1}{4}(|H\rangle + |V\rangle)_1(|H\rangle + |V\rangle)_2(|0000\rangle + |1111\rangle)_{a_1b_1a_2b_2} \\ & + \frac{1}{4}(|H\rangle - |V\rangle)_1(|H\rangle - |V\rangle)_2(|0011\rangle + |1100\rangle)_{a_1b_1a_2b_2}. \end{aligned} \quad (19)$$

From Eq. (19), one can see that either the single-photon detectors D_3D_6 click or the detectors D_2D_5 click. Similarly, the measurement of the other three cases is shown in Table II. With the outcomes of four detectors, we can distill $|\phi^+\rangle_{a_1b_1}|\phi^+\rangle_{a_2b_2}$ and $|\psi^+\rangle_{a_1b_1}|\psi^+\rangle_{a_2b_2}$ from the four cases discussed above.

TABLE II: The results of the four single-photon detectors corresponding to the initial entangled states of the four atoms.

Initial states	Photons measurement		
	(a_1b_1)	(a_2b_2)	Detector click
$ \phi^+\rangle$	$ \phi^+\rangle$	D_3D_6	or D_2D_5
$ \phi^+\rangle$	$ \psi^+\rangle$	D_3D_5	or D_2D_6
$ \psi^+\rangle$	$ \phi^+\rangle$	D_3D_5	or D_2D_6
$ \psi^+\rangle$	$ \psi^+\rangle$	D_3D_6	or D_2D_5

Third, to recover the entangled states of atoms a_1 and b_1 , Alice and Bob should perform a Hadamard operation H_a on the two nonlocal atoms a_2 and b_2 in the waveguides, respectively. Then, Alice and Bob measure the states of the two atoms a_2 and b_2 , and compare their results with the help of classical communication. If the results are the same ones, nothing needs to be done; otherwise, a σ_z operation needs to be put on atom a_1 . From Table II, one can see that there are two cases in the reserved entangled pairs a_1 and b_1 . One is $|\phi^+\rangle_{a_1b_1}$ with a probability of F^2 , and the other one is $|\psi^+\rangle_{a_1b_1}$ with a

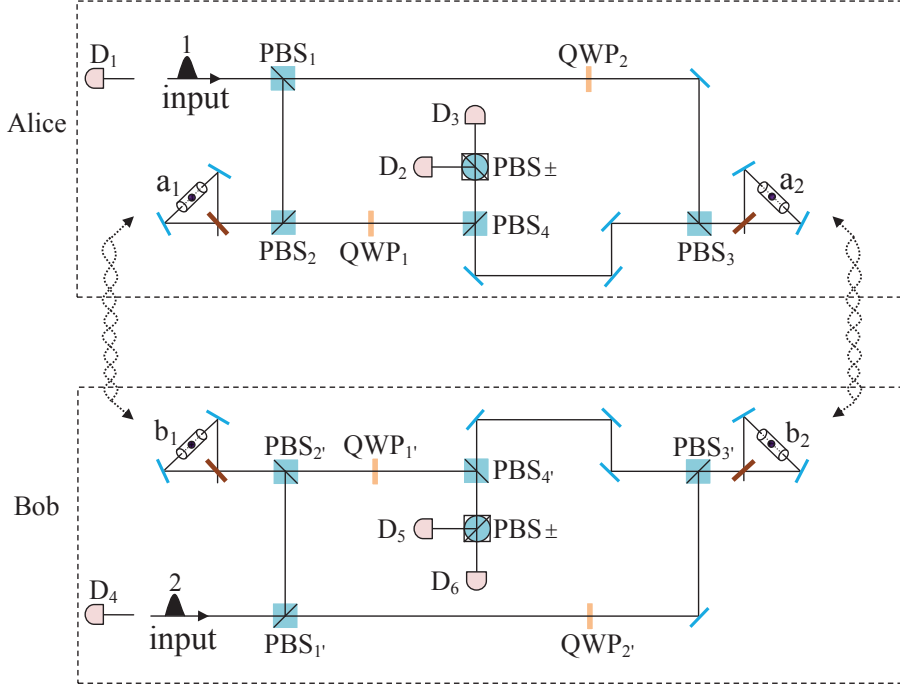


FIG. 4: Schematic setup showing the principle of the atomic entanglement purification protocol based on the scattering of photons off single emitters.

probability of $(1 - F)^2$. Therefore, in the filtered states, the probability of $|\phi^+\rangle_{a_1 b_1}$ is

$$F' = \frac{F^2}{F^2 + (1 - F)^2}. \quad (20)$$

That is, after the purification process, the fidelity of $|\phi^+\rangle_{a_1 b_1}$ becomes F' . When $F > \frac{1}{2}$, one can easily get $F' > F$.

III. DISCUSSION AND SUMMARY

We have proposed a heralded scheme for quantum repeater, including robust nonlocal entanglement creation against collective noise, entanglement swapping, and entanglement purification modules. The key element in our protocol is the scattering process between photons and atoms in 1D waveguides. In the following section, we will discuss the performance of our quantum repeater under practical conditions, defining $p_s = |\langle \psi | \phi_r \rangle|^2$ as the success probability of the scattering event in the protocol of Z gate on an atom, as shown in Fig. 1(b). Here $|\psi\rangle$ and $|\phi_r\rangle$ are the spatial wave functions of the incident photon and the reflected photon component after the scattering event, respectively. For perfect scattering event (i.e., $P \rightarrow \infty$), $|\phi_r\rangle = -|\psi\rangle$, and the success probability p_s is 100%. Whereas, in realistic situations, with finite P , $|\phi_r\rangle \neq -|\psi\rangle$, it includes two cases: one is the successful event of imperfect processes, where the

polarization of output photon is changed but $|\phi_r\rangle = r|\psi\rangle$ ($|r| < 1$); the other one is that the scattering event between atoms and photons does not happen at all. For the latter case, the output photons with unchanged polarization are detected at the entrance, and the corresponding quantum computation is discarded. Assuming that the linear optical elements are perfect in our protocols, the heralded mechanism ensures that the faulty events cannot influence the fidelity of our scheme, but decrease the efficiency, because the success probability p_s is determined by the quality of the atom-waveguide systems.

As mentioned above, a high Purcell factor is needed in our scheme, which can effectively improve the performance of our protocols. In the last decade, a great progress has been made in the emitter-waveguide systems in experiment. In 2006, Chang *et al.* [46] presented a scheme that a dipole emitter is coupled to a nanowire or a metallic nanotip, in which a Purcell factor $P = 5.2 \times 10^2$ is obtained for a silver nanowire. Subsequently, using the surface plasmons of a conducting nanowire, Chang *et al.* [31] obtained an effective Purcell factor, which can reach 10^3 in realistic systems. In addition, short waveguide lengths of only 10 to 20 unit cells were found by Manga Rao and Hughes [47] to produce very large Purcell factors in 2007. Later, based on modifying photon fields around an emitter using high-finesse optical cavities, Akimov *et al.* [48] demonstrated a broadband approach for manipulating photon-emitter interactions. In 2008, photonic crystal waveguides were exploited by Hansen *et al.* [49] to enable a single atom

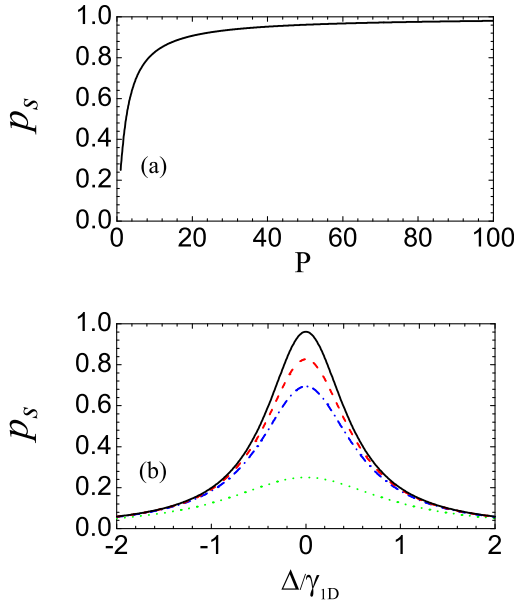


FIG. 5: The success probability p_s of the scattering process vs the Purcell factor P and the detuning parameter Δ/γ_{1D} . (a) The success probability p_s vs the Purcell factor P when the detuning $\Delta = 0$. (b) The success probability p_s vs the parameters Δ/γ_{1D} . The dotted (green), dashed-dotted (blue), dashed (red), and solid (black) lines correspond to $P=1$, $P=5$, $P=10$, and $P=50$, respectively.

to exhibit nearly perfect emission into the guided modes ($\gamma_{1D} \gg \gamma'$) and to act as a highly reflective mirror, where the light-matter coupling strength is largely enhanced. In 2012, Goban [50] reported the experimental implementation of a state-insensitive, compensated optical trap for single Cs atoms, which provides the precise atomic spectroscopy near dielectric surfaces. Moreover, in 2013, Hung *et al.* [51] proposed a protocol in which one atom trapped in single nanobeam structure could provide a resonant probe with transmission $|t|^2 \leq 10^{-2}$. A similar scheme was realized in experiment by Goban *et al.* [52] in 2014. Recently, due to the coupling of a single emitter to a dielectric slot waveguide, a high Purcell factor was also obtained by Kolchin *et al.* [53].

As illustrated in Sec. II A, we can obtain the reflection coefficient for an incident photon scattering with an atom in the 1D waveguide. On resonance, $r = -1/(1 + 1/P)$, and we get the relation between the success probability p_s (i.e., $|r|^2$) and the Purcell factor P , as shown in Fig. 5(a). Moreover, the scattering quality is also influenced by the nonzero photonic detuning, and the details are described in Fig. 5(b), where p_s is plotted as a function of the detuning parameter Δ/γ_{1D} . From Fig. 5, one can see that the success probability p_s would exceed 90% on the condition that the Purcell factor $P \geq 50$ and the detuning parameter $\Delta/\gamma_{1D} \leq 0.13$, which could be easily realized in realistic systems [31]. For instance, when we choose

$P = 100$ and $\Delta = 0.1\gamma_{1D}$ for atom-waveguide systems, the success probability p_s of the scattering process in Fig. 1(b) can reach 94.3%. In detail, for the entanglement creation protocol in our scheme, the incident photon scatters with the atoms twice in 1D waveguides, so the success probability is $(94.33\%)^2 = 88.98\%$, while for both entanglement swapping and entanglement purification protocols, the scattering process occurs four times, and the success rates for them are both $(94.33\%)^4 = 79.18\%$. Considering the influence of other factors, such as photon loss in fiber and defective linear optical elements, the efficiency of our scheme may be low, but this issue can be well solved by the highly efficient single-photon source [54], which provides 10000 single photons per second. Thus, we are able to accomplish our scheme in a short time.

Compared with other schemes, the protocols we present for the heralded quantum repeater have some interesting features. (1) Different from the previous works for quantum repeaters [14–16, 55], in our scheme, the faulty events caused by frequency mismatches, weak coupling, atomic decay into free space, or finite bandwidth of the incident photon can be turned into detection of the output photon polarization, and it just affects the efficiency of our protocols but not the fidelity. In other words, our scheme either succeeds with a perfect fidelity or fails in a heralded way, which is an advantageous feature for quantum communication. (2) In contrast to strong-coupling regime [26, 27, 29, 56, 57], our scheme focuses on Purcell regime [37, 58], where a four-level atom is either embedded in the waveguide or side-coupled to the waveguide, which can be thought of as a bad cavity. It is interesting that the nonlinear optical property can still be obtained in the weak-coupling regime (low-Q regime), which provides an exciting possibility for realistic long-distance quantum communication and quantum information processing [32, 35–37, 58–61]. (3) Motivated by recent experimental progress, our scheme for the heralded quantum repeater is feasible in other related quantum systems, such as superconducting quantum circuit coupled to transmission lines [62–65], quantum dot embedded in a nanowire [66], and photonic crystal waveguide with quantum dots [49, 67].

In summary, we have proposed a heralded quantum repeater based on the scattering of photons off single emitters in 1D waveguides. The information of the entangled states is encoded on four-level atoms embedded in 1D waveguides. As our protocols can transform faulty events into the detection of photon polarization, we present a different way for constructing quantum repeaters in solid-state quantum systems. With the significant progress on manipulating atom-waveguide systems, our quantum repeater may be very useful for quantum communication in the future.

ACKNOWLEDGMENTS

This work was supported by the National Natural Science Foundation of China under Grant No. 11474026, No. 11174040, No. 11475021, and No. 11505007, the Fundamental Research Funds for the Central Universities under Grant No. 2015KJJCA01, the National

Key Basic Research Program of China under Grant No. 2013CB922000, the Youth Scholars Program of Beijing Normal University under Grant No. 2014NT28, and the Open Research Fund Program of the State Key Laboratory of Low-Dimensional Quantum Physics, Tsinghua University Grant No. KF201502.

[1] A. K. Ekert, Phys. Rev. Lett. **67**, 661 (1991).
[2] C. H. Bennett, G. Brassard, and N. D. Mermin, Phys. Rev. Lett. **68**, 557 (1992).
[3] X. H. Li, F. G. Deng, and H. Y. Zhou, Phys. Rev. A **78**, 022321 (2008).
[4] M. Hillery, V. Buzek, and A. Berthiaume, Phys. Rev. A **59**, 1829 (1999).
[5] A. Karlsson, M. Koashi, and N. Imoto, Phys. Rev. A **59**, 162 (1999).
[6] L. Xiao, G. L. Long, F. G. Deng, and J. W. Pan, Phys. Rev. A **69**, 052307 (2004).
[7] G. L. Long and X. S. Liu, Phys. Rev. A **65**, 032302 (2002).
[8] F. G. Deng, G. L. Long, and X. S. Liu, Phys. Rev. A **68**, 042317 (2003).
[9] F. G. Deng and G. L. Long, Phys. Rev. A **69**, 052319 (2004).
[10] H. J. Briegel, W. Dür, J. I. Cirac, and P. Zoller, Phys. Rev. Lett. **81**, 5932 (1998).
[11] M. Żukowski, A. Zeilinger, M. A. Horne, and A. K. Ekert, Phys. Rev. Lett. **71**, 4287 (1993).
[12] D. Deutsch, A. Ekert, R. Jozsa, C. Macchiavello, S. Popescu, and A. Sanpera, Phys. Rev. Lett. **77**, 2818 (1996).
[13] C. H. Bennett, G. Brassard, C. Crepeau, R. Jozsa, A. Peres, and W. K. Wootters, Phys. Rev. Lett. **70**, 1895 (1993).
[14] L. M. Duan, M. D. Lukin, J. I. Cirac, and P. Zoller, Nature (London) **414**, 413 (2001).
[15] A. Klein, U. Dorner, C. M. Alves, and D. Jaksch, Phys. Rev. A **73**, 012332 (2006).
[16] B. Zhao, Z. B. Chen, Y. A. Chen, J. Schmiedmayer, and J. W. Pan, Phys. Rev. Lett. **98**, 240502 (2007).
[17] T. J. Wang, S. Y. Song, and G. L. Long, Phys. Rev. A **85**, 062311 (2012).
[18] T. Li and F. G. Deng, Sci. Rep. **5**, 15610 (2015).
[19] T. Li, G. J. Yang, and F. G. Deng, Phys. Rev. A **93**, 012302 (2015).
[20] Z. Zhao, T. Yang, Y. A. Chen, A. N. Zhang, and J. W. Pan, Phys. Rev. Lett. **90**, 207901 (2003).
[21] A. Kuzmich, W. P. Bowen, A. D. Boozer, A. Boca, C. W. Chou, L. M. Duan, and H. J. Kimble, Nature (London) **423**, 731 (2003).
[22] Z. S. Yuan, Y. A. Chen, B. Zhao, S. Chen, J. Schmiedmayer, and J. W. Pan, Nature (London) **454**, 1098 (2008).
[23] N. Curtz, R. Thew, C. Simon, N. Gisin, and H. Zbinden, Opt. Express **18**, 22099 (2010).
[24] N. Sangouard, C. Simon, H. de Riedmatten, and N. Gisin, Rev. Mod. Phys. **83**, 33 (2011).
[25] K. Hammerer, A. S. Sørensen, and E. S. Polzik, Rev. Mod. Phys. **82**, 1041 (2010).
[26] J. I. Cirac, P. Zoller, H. J. Kimble, and H. Mabuchi, Phys. Rev. Lett. **78**, 3221 (1997).
[27] T. Wilk, S. C. Webster, H. P. Specht, G. Rempe, and A. Kuhn, Phys. Rev. Lett. **98**, 063601 (2007).
[28] D. L. Moehring, P. Maunz, S. Olmschenk, K. C. Younge, D. N. Matsukevich, L. M. Duan, and C. Monroe, Nature (London) **449**, 68 (2007).
[29] Y. Li, L. Aolita, and L. C. Kwek, Phys. Rev. A **83**, 032313 (2011).
[30] J. T. Shen and S. Fan, Opt. Lett. **30**, 2001 (2005).
[31] D. E. Chang, A. S. Sørensen, E. A. Demler, and M. D. Lukin, Nat. Phys. **3**, 807 (2007).
[32] K. Kojima, H. F. Hofmann, S. Takeuchi, and K. Sasaki, Phys. Rev. A **68**, 013803 (2003).
[33] T. C. H. Liew and V. Savona, Phys. Rev. A **85**, 050301(R) (2012).
[34] M. C. Kuzyk, S. J. van Enk, and H. Wang, Phys. Rev. A **88**, 062341 (2013).
[35] M. Bajcsy, S. Hofferberth, V. Balic, T. Peyronel, M. Hafezi, A. Zibrov, V. Vuletic, and M. D. Lukin, Phys. Rev. Lett. **102**, 203902 (2009).
[36] B. C. Ren, G. Y. Wang, and F. G. Deng, Phys. Rev. A **91**, 032328 (2015).
[37] E. Waks and J. Vuckovic, Phys. Rev. Lett. **96**, 153601 (2006).
[38] J. H. An, M. Feng, and C. H. Oh, Phys. Rev. A **79**, 032303 (2009).
[39] Y. Li, L. Aolita, D. E. Chang, and L. C. Kwek, Phys. Rev. Lett. **109**, 160504 (2012).
[40] D. Kalamidas, Phys. Lett. A **343**, 331 (2005).
[41] T. Yamamoto, J. Shimamura, S. K. Özdemir, M. Koashi, and N. Imoto, Phys. Rev. Lett. **95**, 040503 (2005).
[42] X. H. Li, F. G. Deng, and H. Y. Zhou, Appl. Phys. Lett. **91**, 144101 (2007).
[43] T. Yamamoto, K. Hayashi, S. K. Ozdemir, M. Koashi, and N. Imoto, Nat. Photon. **2**, 488 (2008).
[44] J. Berezovsky, M. H. Mikkelsen, N. G. Stoltz, L. A. Coldren, and D. D. Awschalom, Science **320**, 349 (2008).
[45] D. Press, T. D. Ladd, B. Y. Zhang, and Y. Yamamoto, Nature (London) **456**, 218 (2008).
[46] D. E. Chang, A. S. Sørensen, P. R. Hemmer, and M. D. Lukin, Phys. Rev. Lett. **97**, 053002 (2006).
[47] V. S. C. Manga Rao and S. Hughes, Phys. Rev. Lett. **99**, 193901 (2007).
[48] A. V. Akimov, A. Mukherjee, C. L. Yu, D. E. Chang, A. S. Zibrov, P. R. Hemmer, H. Park, and M. D. Lukin, Nature **450**, 402 (2007).
[49] T. Lund-Hansen, S. Stobbe, B. Julsgaard, H. Thyrrstrup, T. Sünner, M. Kamp, A. Forchel, and P. Lodahl, Phys. Rev. Lett. **101**, 113903 (2008).
[50] A. Goban, K. S. Choi, D. J. Alton, D. Ding, C. Lacroute, M. Pototschnig, T. Thiele, N. P. Stern, and H. J. Kimble,

Phys. Rev. Lett. **109**, 033603 (2012).

[51] C. L. Hung, S. M. Meenehan, D. E. Chang, O. Painter, and H. J. Kimble, New J. Phys. **15**, 083026 (2013).

[52] A. Goban, C. L. Hung, S. P. Yu, J. D. Hood, J. A. Muniz, J. H. Lee, M. J. Martin, A. C. McClung, K. S. Choi, D. E. Chang, O. Painter, and H. J. Kimble, Nat. Commun. **5**, 3808 (2014).

[53] P. Kolchin, N. Pholchai, M. H. Mikkelsen, J. Oh, S. Ota, M. S. Islam, X. B. Yin, and X. Zhang, Nano Lett. **15**, 464 (2015).

[54] M. Hijkema, B. Weber, H. P. Specht, S. C. Webster, A. Kuhn, and G. Rempe, Nat. Phys. **3**, 253 (2007).

[55] Z. B. Chen, B. Zhao, Y. A. Chen, J. Schmiedmayer, and J. W. Pan, Phys. Rev. A **76**, 022329 (2007).

[56] H. J. Kimble, Nature (London) **453**, 1023 (2008).

[57] N. H. Lindner and T. Rudolph, Phys. Rev. Lett. **103**, 113602 (2009).

[58] C. Bonato, F. Haupt, S. S. R. Oemrawsingh, J. Gudat, D. Ding, M. P. van Exter, and D. Bouwmeester, Phys. Rev. Lett. **104**, 160503 (2010).

[59] C. H. Bennett and S. J. Wiesner, Phys. Rev. Lett. **69**, 2881 (1992).

[60] X. S. Liu, G. L. Long, D. M. Tong, and L. Feng, Phys. Rev. A **65**, 022304 (2002).

[61] A. Auffèves-Garnier, C. Simon, J. M. Gérard, and J. P. Poizat, Phys. Rev. A **75**, 053823 (2007).

[62] A. A. Abdumalikov Jr., O. Astafiev, A. M. Zagoskin, Yu. A. Pashkin, Y. Nakamura, and J. S. Tsai, Phys. Rev. Lett. **104**, 193601 (2010).

[63] I. C. Hoi, C. M. Wilson, G. Johansson, T. Palomaki, B. Peropadre, and P. Delsing, Phys. Rev. Lett. **107**, 073601 (2011).

[64] I. C. Hoi, T. Palomaki, J. Lindkvist, G. Johansson, P. Delsing, and C. M. Wilson, Phys. Rev. Lett. **108**, 263601 (2012).

[65] A. F. van Loo, A. Fedorov, K. Lalumière, B. C. Sanders, A. Blais, and A. Wallraff, Science **342**, 1494 (2013).

[66] M. Munsch, J. Claudon, J. Bleuse, N. S. Malik, E. Dupuy, J. M. Gérard, Y. Chen, N. Gregersen, and J. Mork, Phys. Rev. Lett. **108**, 077405 (2012).

[67] M. Arcari, I. Söllner, A. Javadi, S. Lindskov Hansen, S. Mahmoodian, J. Liu, H. Thyrrstrup, E. H. Lee, J. D. Song, S. Stobbe, and P. Lodahl, Phys. Rev. Lett. **113**, 093603 (2014).